5-2022

Analysis of Botulinum Toxin A and Interacting Proteins in Skeletal Muscle Cells: An Investigation into the Mechanisms behind Botulinum Toxin A as a Treatment for Chronic Exertional Compartment Syndrome

Lauren Kee
laurenkee23@gmail.com

ANALYSIS OF BOTULINUM TOXIN A AND INTERACTING PROTEINS IN SKELETAL MUSCLE CELLS: AN INVESTIGATION INTO THE MECHANISMS OF BOTULINUM TOXIN A AS A TREATMENT FOR CHRONIC EXERTIONAL COMPARTMENT SYNDROME

By

Lauren R. Kee

Honors Scholarship Project

Submitted to the Faculty of

Olivet Nazarene University

for partial fulfillment of the requirements for

GRADUATION WITH UNIVERSITY HONORS

February 16, 2022

BACHELOR OF SCIENCE

in

Chemistry; Concentration in Biochemistry

Willa S. Harper	Willa S. Harper	2/15/22
Scholarship Project Advisor (printed)	Signature	Date
Stephen Cook		4.27.22
Honors Council Chair (printed)	Signature	Date
Daniel Sharda		4/27/22
Honors Council Member (printed)	Signature	Date

ACKNOWLEDGEMENTS

I would like to thank my mentor, Dr. Harper, for her support, encouragement, and guidance throughout this research process. Thanks also to Dr. Heyen for his assistance and advice on my project, especially with statistical analysis. I would also like to thank the Pence-Boyce Undergraduate Summer Research Program, Honors Department, and Chemistry and Geosciences Department of Olivet Nazarene University for providing financial support for my research. Finally, thank you to Dr. Case, Dr. Stipp, Dr. Ingram, Dr. Schurman, Dr. Sharda, and Dr. Vander Schaaf for investing in me and this project, as well as my roommates, Megan Drenth and Rachel Meyer, and friends in Cohort 12 for their solidarity and motivation throughout my time in the ONU Honors Program.

TABLE OF CONTENTS

LIST OF FIGURES

LIST OF TABLES

ABSTRACT

Background: Chronic exertional compartment syndrome (CECS) is a condition in which muscle tissue expands against the surrounding fascia during activity and is compressed along with the nerves and blood vessels within the muscle compartment, leading to abnormally high intracompartmental pressure (ICP) and debilitating pain. Treatment typically includes fasciotomy, which results in significant levels of CECS recurrence; however, botulinum toxin A (BoNT-A) injection has recently been seen to decrease both ICP and pain through an unknown mechanism with little to no recurrence.

Methods: In this study, PyRosetta was used to model the probability of docking interaction between BoNT-A light or heavy chain and enzymes cyclooxygenase-1 (COX-1), cyclooxygenase-2 (COX-2), prostaglandin E_2 receptor 4 (EP4), endothelial nitric oxide synthase (eNOS), and inducible nitric oxide synthase (iNOS). Subsequently, myoblasts (HSkM) were treated with BoNT-A and assayed based on PyRosetta predicted interactions.

Results: The EP4/BoNT-A heavy chain combination was found to have reaction scores most comparable to known interactions of BoNT-A in neural cells. In accordance with this finding, levels of cyclic adenosine monophosphate (cAMP), a downstream effector of EP4, consistently increased in myoblasts treated with BoNT-A.

Conclusion: Altogether, these data uncover an area of future research in determining the interaction of BoNT-A and the EP4 pathway in muscle cells, as well as the implications this may have on CECS and its treatment.

Keywords: chronic exertional compartment syndrome, CECS, botulinum toxin A, BoNT-A, Botox, prostaglandin E_2 receptor 4, EP4, cyclooxygenase-1, COX-1, cyclooxygenase-

2, COX-2, endothelial nitric oxide synthase, eNOS, inducible nitric oxide synthase, iNOS, cyclic adenosine monophosphate, cAMP, human skeletal muscle myoblast, PyRosetta

INTRODUCTION

Chronic exertional compartment syndrome (CECS) is a condition in which muscle tissue expands against the surrounding fascia during activity and is compressed along with the nerves and blood vessels within the muscle compartment leading to abnormally high intracompartmental pressure (ICP). Proposed causes of CECS include ischemia, muscle hypertrophy, and fascial resistance or hypersensitivity, although the triggers are unknown. This condition is characterized by debilitating pain and cramping of the affected muscles during exercise that is relieved quickly with rest, and diagnosis is based on occurrence of these symptoms and high ICP measurements shortly post-activity. Typical treatment involves cessation of activity or fasciotomy, both of which have high levels of CECS recurrence that vary significantly between various studies but are often 20-50% (Wuellner, et al., 2017).

REVIEW OF LITERATURE

BoNT-A as a Treatment for Chronic Exertional Compartment Syndrome

Botulinum toxin A (BoNT-A) has recently been demonstrated to reduce symptoms of CECS and ICP levels when injected into the affected muscles, but the mechanisms behind this treatment are not well understood. In one study, 15 out of 16 patients diagnosed with CECS and treated with BoNT-A had reduced pain and normal ICP during activity 3 to 9 months post-injection. Proposed causes for symptom relief include reduced release of acetylcholine (causing muscle atrophy), reduction of muscle hypotonia, and/or induced muscle relaxation leading to increased blood flow to the affected muscles (Isner-Horobeti, et al., 2013). Another case study demonstrated long-lasting relief of severe CECS symptoms with BoNT-A injection, with ultrasound showing

no signs of muscle atrophy or texture changes (Baria & Sellon, 2016). This challenges previously accepted assumptions that ICP decrease is due to atrophy of the injected muscles and indicates that another mechanism of BoNT-A is present, potentially at the cellular, neural, or vascular level. Finally, a case study of CECS in the hand demonstrated reduced ICP, full strength recovery, and decreased hypertrophy 15 months post-injection; and the mechanisms of BoNT-A hypothesized were amyotrophy due to reduction of acetylcholine (ACh) release, improved blood supply to limit muscle ischemia, and analgesic action (Orta, et al., 2018). However, not all of these mechanisms would decrease ICP, so the researchers suggested that these effects might be combined with each other or work in addition to other mechanisms. Thus, the exact mechanisms of BoNT-A on CECS symptom management remains unclear and highlights areas for further research.

Mechanisms of Botulinum Toxin Type A

BoNT-A is most understood through its application at the neuromuscular junction. In normal activity of the neuromuscular junction, muscle contraction is initiated as synaptic vesicles filled with ACh are released via exocytosis across the nerve-muscle synapse. In order for this to occur, synaptic vessels are loaded and docked onto the presynaptic membrane, where they are primed by ATP so that they can undergo calcium-regulated exocytosis. Soluble NSF (N-ethylmaleimide sensitive factor) attachment protein (SNAP) receptors (SNAREs) are essential to transporting the vesicle membrane near the plasma membrane, and dissociation of the SNARE complex by binding of SNAPs and NSF is necessary for this process to be carried out (Dolly, 2003).

When neural cells are treated with BoNT-A, the heavy chain of BoNT-A binds to distinct G-protein coupled receptors (GPCRs) on the cell membrane. This allows the toxin to enter the cytosol, where the SNAP-25 protein is cleaved by the light chain of BoNT-A, which contains a selective, zinc-dependent protease. Therefore, the release of ACh from peripheral nerves is inhibited. This blockage of ACh is typically long-lasting and highly selective, and beneficial effects may last three to six months depending on the condition being treated (Dolly, 2003). However, the effect of BoNT-A outside of the neuromuscular junction is not well understood or researched, although other potential applications include its antinociceptive and anti-inflammatory effects (Aoki, 2005; Matak, et al., 2019). As discussed previously, researchers who have treated CECS with BoNT-A have proposed interactions between BoNT-A and skeletal muscle at the cellular, neural, or vascular levels. These interactions may replace or occur in addition to the interaction at the neuromuscular junction (Baria & Sellon, 2016; Isner-Horobeti, et al., 2013; Orta, et al., 2018).

Relevant Pathways and Receptors within Skeletal Muscle

Since BoNT-A interacts at the neuromuscular junction through a GPCR, it is possible that BoNT-A may interact with other GPCRs present on skeletal muscle cells and cause downstream effects or enter the cell and affect intracellular proteins. Many prostaglandins (PGs), which are synthesized through the cyclooxygenase (COX) pathway, as well as endothelial and inducible nitric oxide synthase (eNOS and iNOS, respectively) are influenced by GPCRs and directly involved in relief and regulation of the symptoms of CECS through regulation of blood flow, inflammation, muscle cell expansion, and nociception (Liu, et al., 2016; Mortensen, González-Alonso, et al., 2007;

Mortensen, Nyberg, et al., 2009; Sun & Ye, 2012). Prostaglandin E_2 receptor 4 (EP4), in particular, is a PG receptor and GPCR that can cause inflammation and be involved in inflammatory diseases and responses, and it activates adenyl cyclase (AC) to upregulate cyclic adenosine monophosphate (cAMP) within the cell. Increases in cAMP can lead to hypertrophic responses of myofibers in skeletal muscle, an issue seen in patients with CECS (Berdeaux & Stewart, 2012; Yokoyama, et al., 2013).

Additionally, novel studies of BoNT-A treatment on chronic visceral pain through injection to peripheral organs have demonstrated inhibition of COX-2 and EP4 expression. When prostatitis was induced in rats, injection of BoNT-A led to an 89.4% decrease of COX-2 expression in the prostate and a 90.5% decrease in the L6 spinal cord (Chuang, et al., 2008). A similar study of BoNT-A injection after induced cystitis in rats found that COX-2 expression was reduced by 77.8%, 61.7%, and 54.8% while EP4 expression was reduced by 56.8%, 26.9%, and 84.2% in the bladder, L6 spinal cord, and S1 spinal cord, respectively. This indicates that BoNT-A inhibits COX-2 and EP4 expression in visceral organs and the L6 and S1 spinal cord and suppresses inflammation and hyperactivity (Chuang, et al., 2009). Another study of BoNT-A treatment on human myoblasts and fibroblasts *in vitro* demonstrated that BoNT-A modulated the cell cycle and transcriptome within myoblasts through direct interactions between the toxin and different cellular surface receptors, intracellular targets, and signaling pathways (Zanotti, et al., 2018).

Altogether, these studies suggest it is reasonable to hypothesize that upregulation of cAMP, EP4, COX-2 and similar proteins such as COX-1, iNOS, or eNOS could cause symptoms of CECS and could therefore be modulated by direct BoNT-A treatment if

BoNT-A can bind to surface protein receptors such as EP4 and inhibit further signaling and activation of cAMP or intracellular proteins such as COX-1, COX-2, iNOS, or eNOS.

Effects of BoNT-A on Human Skeletal Muscle Cells *in vitro*

Therefore, the present study aimed to determine if COX-1, COX-2, eNOS, iNOS, or EP4 are likely to interact directly with BoNT-A, by creating and analyzing protein models using protein-protein and protein-ligand docking programs from PyRosetta, a computational chemistry program. These results indicated an interaction between BoNT-A heavy chain and EP4, which was subsequently confirmed as levels of cAMP in human skeletal muscle myoblasts increased after treatment with BoNT-A.

METHODS

Computational Analysis

In order to analyze probability of interaction between BoNT-A light chain (LC) or heavy chain (HC) and COX-1, COX-2, eNOS, iNOS, or EP4, protein and ligand structures were first obtained from the Protein Data Bank (PDB). The specific PDB IDs used were 2IMC for BoNT-A LC (Silvaggi, et al. 2007), 2VUA for BoNT-A HC (Stenmark, et al. 2008), 6Y3C for COX-1 (Miciaccia, et al., 2021), 5IKR for COX-2 (Orlando & Malkowski, 2016), 4D1O for eNOS (Li, et al., 2014), 2NSI for iNOS (Li, et al.,1999), and 7D7M for EP4 (Nojima, et al., 2021). BoNT-A LC was combined with COX-1, COX-2, iNOS, and eNOS based on their location within the cell cytoplasm and the mechanism of BoNT-A LC within the cell, while BoNT-A HC was combined with EP4 based on its location within the cell membrane and the mechanism of BoNT-A HC to bind and allow entrance into the cell. BoNT-A LC was also combined with

synaptosome associated protein 25 (SNAP25) (PDB ID: 3DDA; Kumaran, et al., 2008), and BoNT-A HC was combined with ganglioside co-receptor GT1B (PDB ID: 2VU9; Stenmark, et al., 2008). These combinations have known interactions *in vivo*, allowing them to be used as control comparisons for output data. Using a virtual machine enabled with PyRosetta (PyRosetta4.Release.python38.inux.release-275; Chadbury, et al., 2010) and PyMOL (The PyMOL Molecular Graphics System, Version 2.0, n.d.), proteins were combined into a joint file, cleaned from additional H_2O or interfering ligand molecules, and filled with any missing amino acid residues. Finally, joint files were run through protein-protein (for all combinations including BoNT-A LC) or protein-ligand (for all combinations including BoNT-A HC) docking programs from PyRosetta software.

Human Skeletal Myoblast Differentiation Culture

After thawing, human skeletal myoblasts (HSkM, Cat. no. A12555 & A11440; Gibco) were differentiated in Dulbecco's Modified Eagle Medium (Gibco) supplemented with 2% horse serum (Gibco), plated on an untreated 24-well plate with a density of 240,000 cells per well, and incubated at 37 °C with 5% CO_2. After 48 hours, HSkM cells became elongated, indicating their differentiation was complete and allowing further treatments to proceed.

Preparation of Botulinum Toxin A Dilutions

An original vial containing 100 IU of BoNT-A (Creative BioMart) was diluted with 5 mL of bacteriostatic 0.9% sodium chloride solution (Hospira) to a concentration of 20 IU/mL. Then, a serial dilution in differentiation medium was made to produce dilutions of 0, 0.24, 0.48, 1.2, 2.4, 4.8, 7.2, and 9.6 IU/mL, which corresponds to 0, 0.5,

1, 2.5, 5, 10, 15, or 20 IU BoNT-A per 10^6 cells, based on the dilutions tested in previous models (Zanotti et al., 2018).

Cytotoxic Assessment with DAPI and PI Fluorescence Assay

After differentiation, cells were treated in triplicate with 0.5 mL per well of either 0, 0.5, 1, 2.5, 5, 10, 15, or 20 IU per 10^6 cells, as prepared above. Cells were incubated at 37 °C with 5% CO_2 for 24 hours, aspirated, stained with a solution containing 1 μL/1 mL 4',6-diamidino-2-phenylindole (DAPI; ThermoFisher) and 1 μL/1 mL propidium iodide (PI; ThermoFisher) in 1X PBS, and incubated for 10 minutes before aspirating and washing twice with 1X PBS. Cells were imaged using a Nikon Ti-E Fluorescent Microscope and counted using cell counting software to determine cytotoxicity of treatments.

cAMP Direct Immunoassay

In order to investigate the effects of BoNT-A on EP4, the levels of cAMP in cells with or without BoNT-A treatment were analyzed through the cAMP Direct Immunoassay Kit (Colorimetric) (Cat. no. K371; BioVision). HSkM were differentiated, treated with either 0 IU (control cells) or 1 IU BoNT-A per 10^6 cells diluted in bacteriostatic 0.9% sodium chloride solution (Hospira) and differentiation medium as prepared above for the cytotoxicity assay, and incubated at 37 °C with 5% CO_2 for 24 hours. Medium was aspirated, and cells were treated with 50 μL of 0.1 M HCl per well and incubated at room temperature. Cells were scraped, collected, and centrifuged, and the supernatant was assayed directly. The standard cAMP curve and quantification of cAMP in samples was achieved following the protocol included in the kit.

Statistical Analysis

Statistical analysis of cAMP concentration data was performed using an F-test and Student's t-test assuming equal variances on Microsoft Excel. Through these tests, both one-tailed and two-tailed p-values were obtained and compared.

RESULTS

Computational Data Indicates HC-EP4 Interaction

Computational data outputs were received as total weighted scores measured in Rosetta Energy Units (REU). These scores had values similar to exothermic and endothermic reaction energy values – thus, more negative values indicated a more stable and therefore more likely interaction between the molecules tested. Each combination tested gave 3-6 scores based on different docking positions. Therefore, an average of these values would not be relevant as each value represented a distinct position of interaction, and only the most probable position of interaction should be considered. The lowest value from each combination was compared in order to determine the most likely interaction to be further tested. As seen in Fig. 1, the total weighted score of HC-EP4 was most comparable to the controls, LC-SNAP25 and HC-GT1B, while other test combinations were significantly different from the controls. The lowest values for control combinations were -585.193 REU and -128.517 REU for LC-SNAP25 and HC-GT1B, respectively, and the lowest value for test combinations was -677.325 REU for HC-EP4 (Table 1). Consequently, EP4 was chosen to be further investigated through its secondary effector, cAMP, during *in vitro* testing.

Table 1: Lowest total weighted scores are predicted by PyRosetta between BoNT-A and SNAP25, EP4, and GT1B.

Docking Combination	Lowest Total Weighted Score (REU)	-log(REU)
LC-SNAP25	-847.419	2.928098
HC-EP4	-735.705	2.866704
HC-GT1B	-128.517	2.108961
LC-iNOS	74243.906	-4.87066
LC-eNOS	74866.516	-4.87429
LC-COX2	77261.938	-4.88797
LC-COX1	78015.531	-4.89218

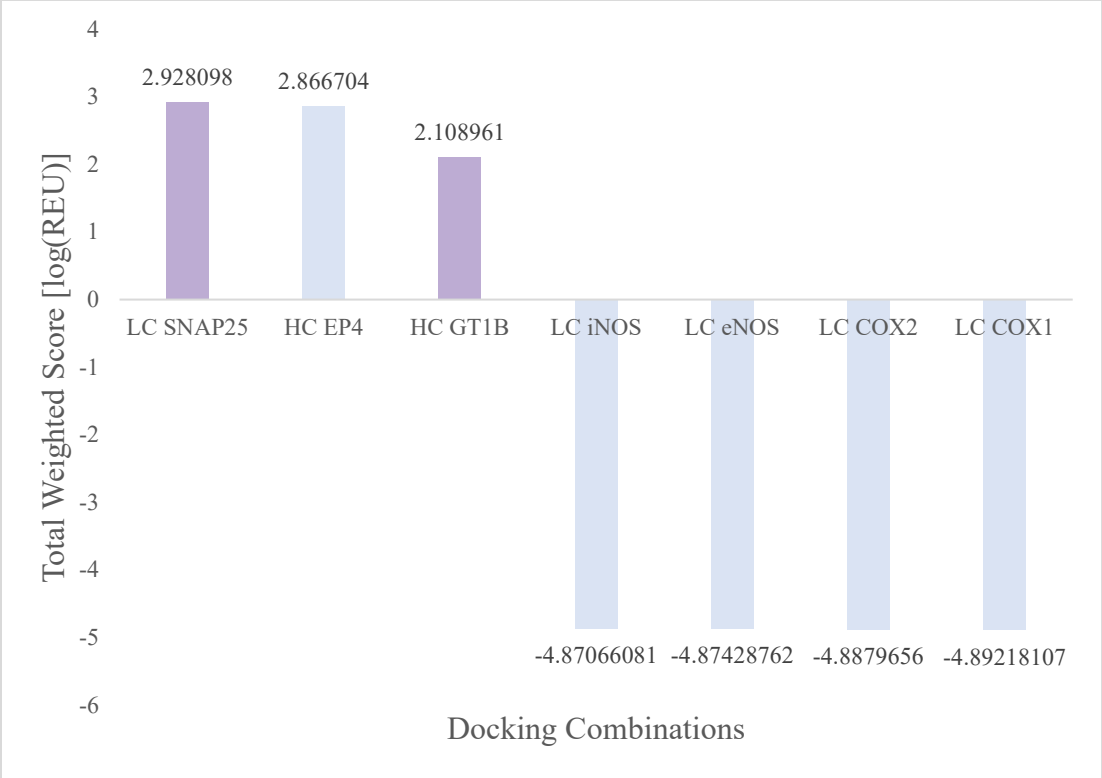

Figure 1: Strong docking interactions are predicted by PyRosetta between BoNT-A and SNAP25, EP4, and GT1B, but not iNOS, eNOS, COX2, or COX1. Combinations are between either BoNT-A light chain (LC) or heavy chain (HC) and SNAP25, EP4, GT1B, iNOS, eNOS, COX2, or COX1 based on their location within the cell. The lowest total weighted score was taken from each combination. If this score was negative, the log of the absolute value was taken. For positive scores, the –log was taken. Therefore, in this graph, a more positive score corresponds with a more probable docking position and interaction. Control combinations are shown in purple, while test combinations are shown in blue.

Cytotoxicity Assessment of HSkM Treated with BoNT-A

Cytotoxicity was determined through fluorescence microscope imaging, as seen in Fig. 2. In Fig. 3, BoNT-A concentrations of 0-5 IU per 10^6 cells were seen to be most consistent at causing minimal cytotoxicity, while concentrations of 10-20 IU per 10^6 cells were more variable. Average cytotoxicity of cells treated with 1 IU BoNT-A was 0.997 ± 1.421%, while average cytotoxicity of cells treated with 20 IU BoNT-A was 80.5 ± 10.5%.

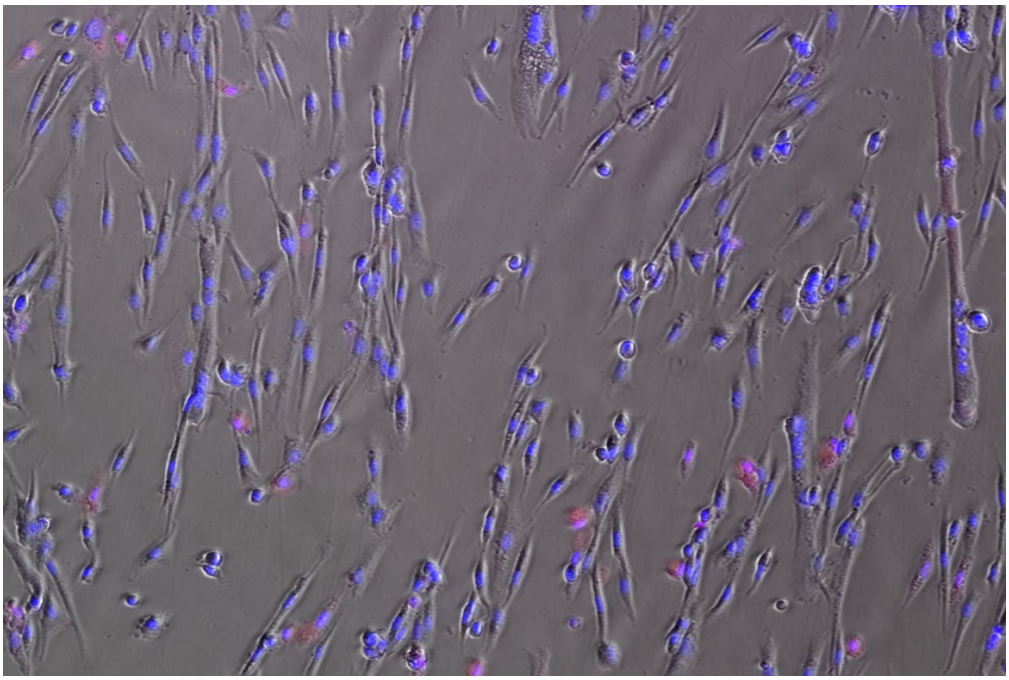

Figure 2: Cell viability of HSkM is not affected by 1 IU of BoNT-A. Fluorescence microscope imaging of HSkM after BoNT-A with DAPI (blue) for viability, and PI (red) for cytotoxicity. Cell counting software identified these colored spots to determine total cell count and total dead cell count.

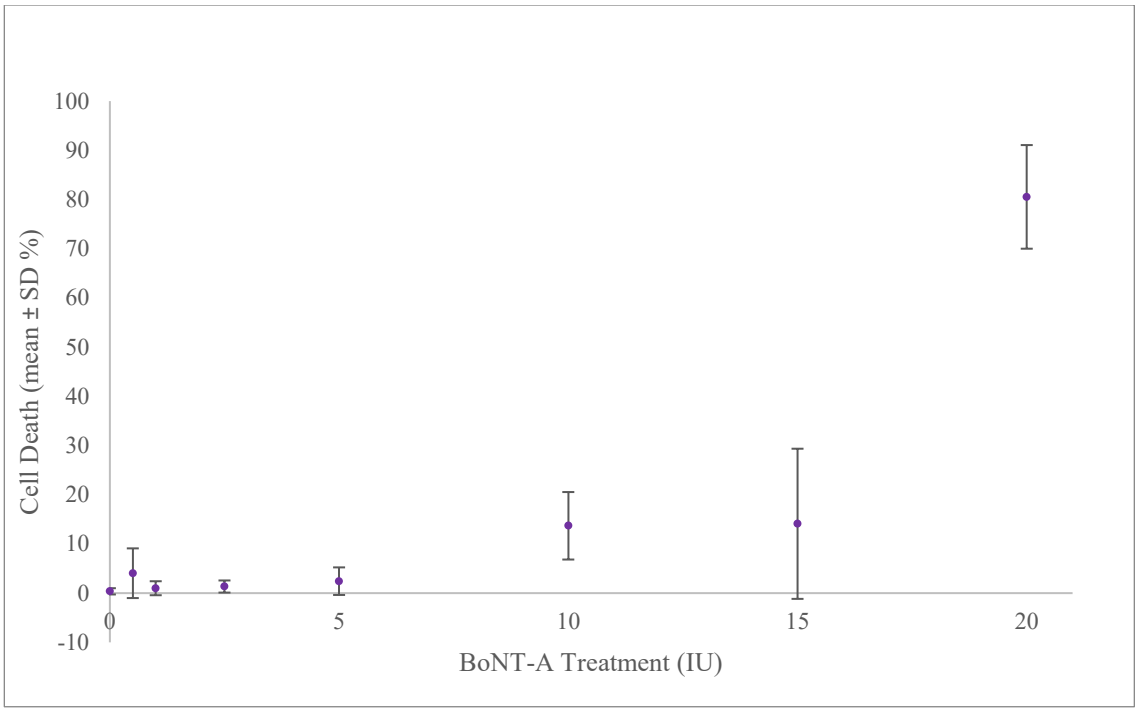

Figure 3: Cytotoxicity of BoNT-A treatment on HSkM myoblasts cells increases progressively with concentration. Concentrations of 0, 0.5, 1, 2.5, 5, 10, 15, and 20 IU BoNT-A per 10^6 cells were incubated at 37 °C with 5% CO_2 for 24 hours, aspirated, stained with DAPI and PI in 1X PBS, and incubated for 10 minutes before aspirating and washing with 1X PBS. Cells were imaged using a Nikon Ti-E Fluorescent Microscope and counted to determine cytotoxicity of treatments. Results shown indicate the mean ± standard deviation of cell death for each treatment.

cAMP Direct Immunoassay

PyRosetta's predicted interaction between BoNT-A HC and EP4 was investigated *in vitro* through activity assessment of cAMP, a secondary messenger of EP4. Based on high cell viability, a treatment of 1 IU BoNT-A per 10^6 cells was selected for analysis with the cAMP direct immunoassay. Control samples had cAMP concentrations of 3.498 fmol/well and 2.665 fmol/well for an average of 3.081 ± 0.589 fmol/well, while the two wells containing samples treated with 1 IU BoNT-A had cAMP concentrations of 9.478 fmol/well and 6.522 fmol/well for an average of 8.000 ± 2.090 fmol/well, showing a

consistent increase in cAMP (Fig. 4). In a two-sample F-test for variances, $F_{stat} < F_{crit}$, indicating that the variances were equal. According to the one-tail two-sample t-test assuming equal variances, $p = 0.04$, indicating that cAMP concentration in cells treated with 1 IU BoNT-A was significantly higher than cAMP concentration in control cells.

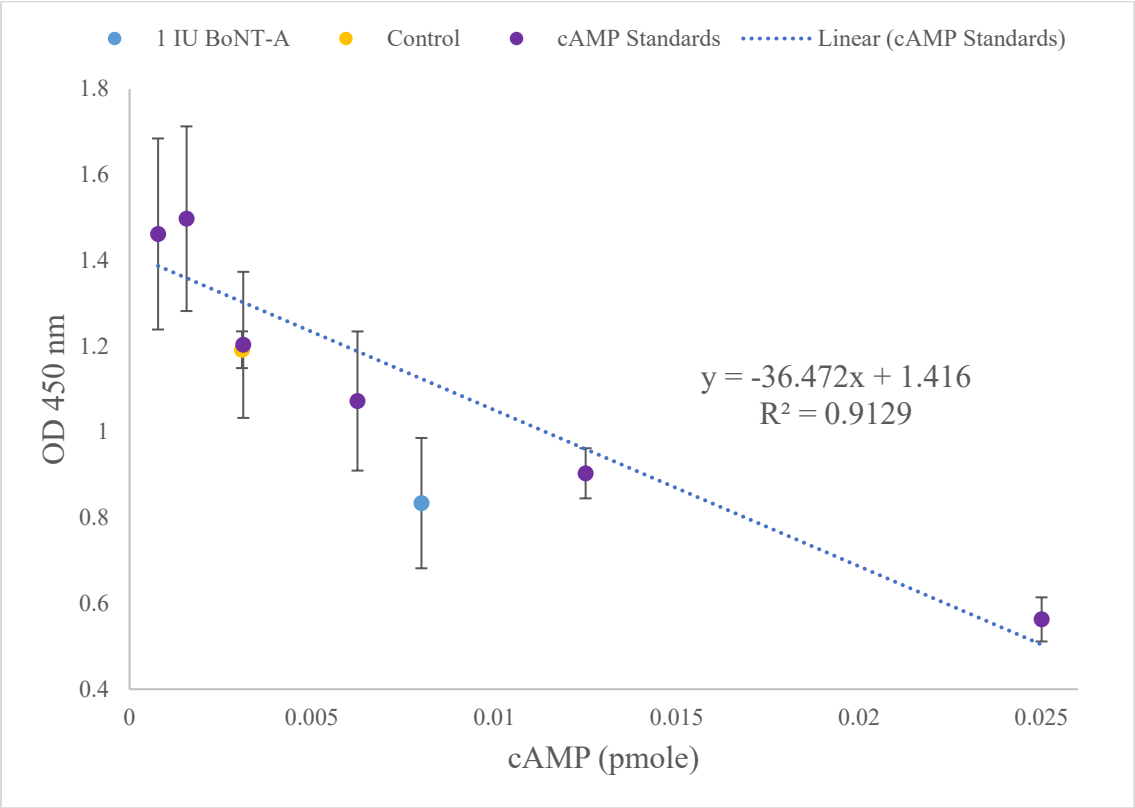

Figure 4: Concentration of cAMP increases with BoNT-A treatment. cAMP standards were used to form a standard curve and regression line. The equation of this line was used to determine cAMP concentration in control and 1 IU BoNT-A treated cells based on OD 450 nm readings, and these data points are also displayed. Data points in purple represent the standard cAMP curve, while the data point in yellow represents the average cAMP in control cells, 3.081 ± 0.589 fmol/well, and the data point in blue represents the average cAMP in cells treated with 1 IU BoNT-A, 8.000 ± 2.090 fmol/well. Results shown indicate the mean ± standard deviation of OD 450 nm readings for each standard, control, and treatment.

DISCUSSION

The results of this research indicate that BoNT-A could likely be interacting with EP4 within HSkM, but the extent and mechanisms of this interaction are still unclear based on this data. Computational analysis suggests that BoNT-A HC and EP4 could

have a stable interaction. While previous data demonstrates that BoNT-A may reduce EP4 expression in the spinal cord and visceral organs (Chuang, et al., 2009), this is the first research to propose direct molecular interactions between EP4 and BoNT-A HC. In contrast, high total weighted scores from BoNT-A LC and COX-1, COX-2, eNOS, and iNOS were significantly less stable. However, previous research indicates BoNT-A does affect COX-2 *in vivo* (Chuang, et al., 2008; Chuang, et al., 2009), so this data could instead imply either no interaction or a momentary, unstable interaction between these molecules. Additionally, these molecules could be affected indirectly, which was not investigated in this study. Finally, this data could also represent a context-dependent interaction, in which BoNT-A may only interact with these molecules under certain cellular conditions, such as the stress of exercise on muscle cells.

Data from the cAMP immunoassay suggests BoNT-A treatment correlates with increased cAMP within HSkM *in vitro*, but more research is needed to determine the significance of this increase, as well as whether different dilutions of BoNT-A result in different increases of cAMP. Because upregulation of cAMP can cause hypertrophy in skeletal muscle myofibers (Berdeax & Stewart, 2012), this data is surprising since BoNT-A treatment *in vivo* leads to reduced hypertrophy in patients with CECS (Baria & Sellon, 2016; Isner-Horobeti, et al., 2013; Orta, et al., 2018). Furthermore, it is unclear whether this increase is caused by activation of EP4 or by a different mechanism as cAMP is involved with many cellular processes. Additionally, this study was limited by a small number of experimental samples, so future research should include a greater number of samples for clearer significance and meaning of results.

The specific interaction of BoNT-A with EP4 is a topic of further investigation regarding the mechanisms of BoNT-A within skeletal muscle. This could be achieved through similar experiments in EP4 knockout mice with cAMP monitoring, as well as experiments involving increased dosage of cAMP and symptom monitoring. Additionally, other studies involving BoNT-A's effects *in vivo* have analyzed the expression of proteins after treatment in both the affected organs and spinal cord, as well as in individual cell transcriptomes (Chuang, et al., 2008; Chuang, et al., 2009; Zanotti, et al., 2018). Therefore, analysis of mRNA and spinal cord protein expression in addition to tracking symptom management after affected skeletal muscle cells are treated with BoNT-A may provide more insight in determining its mechanism in relation to its therapeutic effects in treating CECS.

Finally, only normal HSkM were examined within this study. Since the mechanisms and progression of CECS in skeletal muscle is largely misunderstood, HSkM affected by CECS could interact with BoNT-A differently than normal HSkM. Thus, further research should include analysis and comparison of cAMP and EP4 expression in both normal and CECS-affected HSkM in order to explore CECS and the causes of this condition.

CONCLUSION

Overall, more data is needed to fully determine the mechanisms and effects of BoNT-A on HSkM *in vitro*, especially in regards to EP4 interaction and cAMP concentration. Most importantly, however, the data from this study indicates BoNT-A may influence skeletal muscle cells outside of its effect at the neuromuscular junction through novel computational evidence of EP4 and BoNT-A HC molecular interaction, as

well as increased levels of cAMP in HSkM treated with BoNT-A, with $p = 0.04$ in the one-tail t-test. Further investigation into the specific results of BoNT-A treatment on skeletal muscle can provide valuable implications to both the uses of BoNT-A as a treatment in a variety of diseases as well as the mechanisms of diseases such as CECS that observe symptom reduction through therapeutic uses of BoNT-A.

REFERENCES

Aoki, K. R. (2005). Review of a Proposed Mechanism for the Antinociceptive Action of Botulinum Toxin Type A. *NeuroToxicology*, *26*(5), 785–793. https://doi.org/10.1016/j.neuro.2005.01.017

Baria, M. R., & Sellon, J. L. (2016). Botulinum toxin for chronic exertional compartment syndrome: A case report with 14 month follow-up. *Clinical Journal of Sports Medicine*, *29*(2), e111–e113. https://doi.org/10.1097/JSM.0000000000000289

Berdeaux, R., & Stewart, R. (2012). cAMP signaling in skeletal muscle adaptation: Hypertrophy, metabolism, and regeneration. *American Journal of Physiology-Endocrinology and Metabolism*, *303*(1), E1–E17. https://doi.org/10.1152/ajpendo.00555.2011

Chadbury, S., Lyskov, S., & Gray, J. J. PyRosetta: a script-based interface for implementing molecular modeling algorithms using Rosetta. *Bioinformatics, 26*(5), 689-691 (2010).

Chuang, Y.-C., Yoshimura, N., Huang, C.-C., Wu, M., Chiang, P.-H., & Chancellor, M. B. (2008). Intraprostatic botulinum toxin a injection inhibits cyclooxygenase-2 expression and suppresses prostatic pain on capsaicin induced prostatitis model in rat. *The Journal of Urology*, *180*(2), 742–748. https://doi.org/10.1016/j.juro.2007.07.120

Chuang, Y.-C., Yoshimura, N., Huang, C.-C., Wu, M., Chiang, P.-H., & Chancellor, M. B. (2009). Intravesical botulinum toxin A administration inhibits COX-2 and EP4 expression and suppresses bladder hyperactivity in cyclophosphamide-induced

cystitis in rats. *European Urology*, *56*(1), 159–167. https://doi.org/10.1016/j.eururo.2008.05.007

Dolly, O. (2003). Synaptic transmission: Inhibition of neurotransmitter release by botulinum toxins. *Headache: The Journal of Head and Face Pain*, *43*(s1), 16–24. https://doi.org/10.1046/j.1526-4610.43.7s.4.x

Isner-Horobeti, M.-E., Dufour, S. P., Blaes, C., & Lecocq, J. (2013). Intramuscular pressure before and after botulinum toxin in chronic exertional compartment syndrome of the leg: A preliminary study. *The American Journal of Sports Medicine*, *41*(11), 2558–2566. https://doi.org/10.1177/0363546513499183

Kumaran, D., Rawat, R., Ahmed, S. A., & Swaminathan, S. (2008). Substrate Binding Mode and Its Implication on Drug Design for Botulinum Neurotoxin A. *PLOS Pathogens*, *4*(9), e1000165. https://doi.org/10.1371/journal.ppat.1000165

Li, H., Jamal, J., Plaza, C., Pineda, S. H., Chreifi, G., Jing, Q., Cinelli, M. A., Silverman, R. B., & Poulos, T. L. (2014). Structures of human constitutive nitric oxide synthases. *Acta Crystallographica Section D: Biological Crystallography*, *70*(10), 2667–2674. https://doi.org/10.1107/S1399004714017064

Li, H., Raman, C. S., Glaser, C. B., Blasko, E., Young, T. A., Parkinson, J. F., Whitlow, M., & Poulos, T. L. (1999). Crystal structures of zinc-free and -bound heme domain of human inducible nitric-oxide synthase. Implications for dimer stability and comparison with endothelial nitric-oxide synthase. *The Journal of Biological Chemistry*, *274*(30), 21276–21284. https://doi.org/10.1074/jbc.274.30.21276

Liu, S. Z., Jemiolo, B., Lavin, K. M., Lester, B. E., Trappe, S. W., & Trappe, T. A. (2016). Prostaglandin E2/cyclooxygenase pathway in human skeletal muscle:

Influence of muscle fiber type and age. *Journal of Applied Physiology (Bethesda, Md. : 1985)*, *120*(5), 546–551. https://doi.org/10.1152/japplphysiol.00396.2015

Matak, I., Bölcskei, K., Bach-Rojecky, L., & Helyes, Z. (2019). Mechanisms of botulinum toxin type A action on pain. *Toxins*, *11*(8). https://doi.org/10.3390/toxins11080459

Miciaccia, M., Belviso, B. D., Iaselli, M., Cingolani, G., Ferorelli, S., Cappellari, M., Loguercio Polosa, P., Perrone, M. G., Caliandro, R., & Scilimati, A. (2021). Three-dimensional structure of human cyclooxygenase (hCOX)-1. *Scientific Reports*, *11*(1), 4312. https://doi.org/10.1038/s41598-021-83438-z

Mortensen, S. P., González-Alonso, J., Damsgaard, R., Saltin, B., & Hellsten, Y. (2007). Inhibition of nitric oxide and prostaglandins, but not endothelial-derived hyperpolarizing factors, reduces blood flow and aerobic energy turnover in the exercising human leg. *The Journal of Physiology*, *581*(Pt 2), 853–861. https://doi.org/10.1113/jphysiol.2006.127423

Mortensen Stefan P., Nyberg Michael, Thaning Pia, Saltin Bengt, & Hellsten Ylva. (2009). Adenosine Contributes to Blood Flow Regulation in the Exercising Human Leg by Increasing Prostaglandin and Nitric Oxide Formation. *Hypertension*, *53*(6), 993–999. https://doi.org/10.1161/HYPERTENSIONAHA.109.130880

Nojima, S., Fujita, Y., Kimura, K. T., Nomura, N., Suno, R., Morimoto, K., Yamamoto, M., Noda, T., Iwata, S., Shigematsu, H., & Kobayashi, T. (2021). Cryo-EM Structure of the Prostaglandin E Receptor EP4 Coupled to G Protein. *Structure*

(London, England: 1993), *29*(3), 252-260.e6. https://doi.org/10.1016/j.str.2020.11.007

Orlando, B. J., & Malkowski, M. G. (2016). Substrate-selective Inhibition of Cyclooxygeanse-2 by Fenamic Acid Derivatives Is Dependent on Peroxide Tone. *The Journal of Biological Chemistry*, *291*(29), 15069–15081. https://doi.org/10.1074/jbc.M116.725713

Orta, C., Petit, J., & Gremeaux, V. (2018). Chronic exertional compartment syndrome in hands successfully treated with botulinum toxin-A: A case. *Annals of Physical and Rehabilitation Medicine*, *61*(3), 183–185. https://doi.org/10.1016/j.rehab.2018.02.006

Silvaggi, N. R., Boldt, G. E., Hixon, M. S., Kennedy, J. P., Tzipori, S., Janda, K. D., & Allen, K. N. (2007). Structures of Clostridium botulinum Neurotoxin Serotype A Light Chain complexed with small-molecule inhibitors highlight active-site flexibility. *Chemistry & Biology*, *14*(5), 533–542. https://doi.org/10.1016/j.chembiol.2007.03.014

Stenmark, P., Dupuy, J., Imamura, A., Kiso, M., & Stevens, R. C. (2008). Crystal Structure of Botulinum Neurotoxin Type A in Complex with the Cell Surface Co-Receptor GT1b—Insight into the Toxin–Neuron Interaction. *PLOS Pathogens*, *4*(8), e1000129. https://doi.org/10.1371/journal.ppat.1000129

Sun, L., & Ye, R. D. (2012). Role of G protein-coupled receptors in inflammation. *Acta Pharmacologica Sinica*, *33*(3), 342–350. https://doi.org/10.1038/aps.2011.200

The PyMOL Molecular Graphics System, Version 2.0 Schrödinger, LLC.

Wuellner, J. C., Nathe, C. D., Kreulen, C., Burnham, K., & Giza, E. (2017). Chronic Exertional Compartment Syndrome: The Athlete's Claudication. *Operative Techniques in Sports Medicine*, *25*(2), 52–58. https://doi.org/10.1053/j.otsm.2017.03.004

Yokoyama, U., Iwatsubo, K., Umemura, M., Fujita, T., & Ishikawa, Y. (2013). The Prostanoid EP4 Receptor and Its Signaling Pathway. *Pharmacological Reviews*, *65*(3), 1010–1052. https://doi.org/10.1124/pr.112.007195

Zanotti, S., Kapetis, D., Gibertini, S., Salerno, F., Ciusani, E., Colombo, C., Gronchi, A., Morandi, L., Mantegazza, R., Molteni, F., & Mora, M. (2018). Botulinum toxin type A affects the transcriptome of cell cultures derived from muscle biopsies of controls and spastic patients. *Toxicology in Vitro*, *50*, 124–136. https://doi.org/10.1016/j.tiv.2018.02.008